

Determination of fluorine atom density in reactive plasmas by vacuum ultraviolet absorption spectroscopy at 95.85 nm

K. Sasaki,^{a)} Y. Kawai, and K. Kadota

Department of Electronics, Nagoya University, Nagoya 464-8603, Japan

(Received 2 June 1998; accepted for publication 21 October 1998)

Vacuum ultraviolet absorption spectroscopy was developed for the measurement of absolute fluorine (F) atom density in reactive plasmas. In order to minimize the influence of radiation trapping (self-absorption) in the light source, fluorescence at a wavelength of 95.85 nm from the F atoms in an electron-cyclotron resonance (ECR) CF₄ plasma, which was operated with a low microwave power (0.1 kW) and a low gas pressure (1 mTorr), was employed as the probe emission. A windowless transmission system for the probe emission was constructed by connecting the ECR light source with the target plasma and the detection system using vacuum tubes having small slits. The connection tubes were differentially evacuated with turbomolecular pumps to prevent neutral particles from passing through between the ECR and target plasmas. The present method was applied to high-density CF₄ and C₄F₈ plasmas produced by helicon-wave discharges. The accuracy of the measurement was examined carefully by evaluating various sources of error. In the present article, we have emphasized the evaluation of the radiation trapping effect in the light source plasma. © 1999 American Institute of Physics. [S0034-6748(99)04401-9]

I. INTRODUCTION

Fluorine (F) atoms are utilized in various ways in material processing using low-temperature reactive plasmas, such as dry etching of Si, SiO₂ and various metals, deposition of insulation films with low dielectric constants, polymer modification, and reactor cleaning. However, F atoms are lacking in reliable diagnostics. Although actinometry is widely used for diagnostics of F atoms,¹ its reliability is questionable in low-pressure, high-density plasma sources which are developed for advanced material processing.² Recently, Nakamura *et al.*³ and Tserepi *et al.*⁴ have succeeded in measuring the absolute F atom density with appearance mass spectrometry. Noncontact optical methods are, however, still attractive for the diagnostics of F atoms in reactive plasmas.

A reliable optical method for the measurements of particle densities in plasmas with good spatial and temporal resolutions is laser-induced fluorescence (LIF) spectroscopy. However, the wavelength obtainable with existing tunable lasers is not short enough to excite F atoms, even if two-photon excitation is applied. Another optical method to determine particle densities is absorption spectroscopy. To detect F atoms by absorption spectroscopy employing a resonance lamp, the most severe technical issue arises from the wavelength of the probe emission. Since the first electronic state of the F atom is located at 12.98 eV above the ground state, the wavelength of the probe emission should be shorter than 100 nm. In this vacuum ultraviolet (VUV) wavelength range, no window materials can be used to separate the light source from the target plasma. Another issue of vacuum ultraviolet absorption spectroscopy (VUVAS) is due to radiation trapping (self-absorption) in the light source. If

the line shape of the probe emission is distorted considerably from the Gaussian profile (Doppler broadening) by radiation trapping, the absolute F atom density determined by VUVAS becomes doubtful in its accuracy.

In the present article, we report VUVAS for measurement of the absolute F atom density in reactive plasmas. The accuracy of the present method was examined by evaluating various sources of error, with emphasis on the radiation trapping effect in the light source. The F atom density was measured in high-density CF₄ and C₄F₈ plasmas produced by helicon-wave discharges. The details of the absolute F atom density and the related reaction kinetics in the CF₄ and C₄F₈ plasmas have already been reported previously.⁵⁻⁷

II. PRINCIPLES OF VUVAS

The basic principle of VUVAS is the same as that of usual absorption spectroscopy using resonance lamps. A conventional theory⁸ can be adopted to derive the absolute F atom density from the absorption A , which is determined from the measurements of the incident and transmitted emission intensities I_0 and I_t , respectively, such that

$$A = 1 - \frac{I_t}{I_0} = \frac{\int E_\nu \{1 - \exp(-k_0 L e^{-\omega^2})\} d\omega}{\int E_\nu d\omega}, \quad (1)$$

where L denotes the absorption length in the target plasma and ω is the normalized frequency given by $\omega = 2\sqrt{\ln 2}(\nu - \nu_0)/\Delta\nu_D$ with ν , ν_0 , and $\Delta\nu_D$ being the real frequency, the line center frequency, and the Doppler linewidth (full width at half maximum) of the absorption line, respectively. The functional form $e^{-\omega^2}$ represents a Gaussian profile characterized by a temperature of absorbing F atoms. The absorption coefficient k_0 is related to the population of F atoms n_F at the lower energy level as follows:

^{a)}Electronic mail: sasaki@nuee.nagoya-u.ac.jp

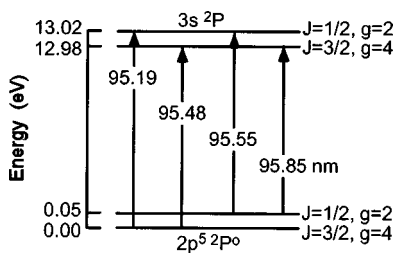


FIG. 1. Partial energy level diagram of F atom.

$$k_0 = \frac{2}{\Delta \nu_D} \sqrt{\frac{\ln 2}{\pi}} \frac{\lambda_0^2}{8\pi} \frac{g_2}{g_1} A_{21} n_F, \quad (2)$$

where λ_0 is the line center wavelength, g_1 and g_2 are the statistical weights of the lower and upper energy levels, respectively, and A_{21} is the transition probability for the related spectral line. The quantity E_ν in Eq. (1) represents the spectral line shape of the probe emission. A Gaussian profile due to Doppler broadening characterized by a temperature of emitting F atoms in the light source is basically adopted for E_ν . However, if radiation trapping (self-absorption) in the light source is strong, the line shape of the probe emission is distorted from the Gaussian profile considerably.

Figure 1 shows the partial energy level diagram of the F atom. Since the ground and first electronic states of the F atom have two sublevels with intervals of 0.05 and 0.04 eV, respectively, the four transition lines shown in Fig. 1 can possibly be used for the absorption measurement. Among the four lines, we have chosen the transition at a wavelength of 95.85 nm ($3s^2 P_{3/2}^{\circ} \leftarrow 2p^5 2P_{1/2}^{\circ}$) as the probe emission because of the reason described in the discussion. With this transition, the density of the upper ground state ($2p^5 2P_{1/2}^{\circ}$) can be obtained. The total density of F atoms at the ground state ($2p^5 2P_{1/2,3/2}^{\circ}$) is evaluated by assuming the Boltzmann distribution between the two sublevels.

III. EXPERIMENT

The experimental apparatus is schematically shown in Fig. 2. Measurement of the F atom density was carried out in a helicon-wave plasma source which had a uniform magnetic field of 1 kG along the cylindrical axis of the vacuum cham-

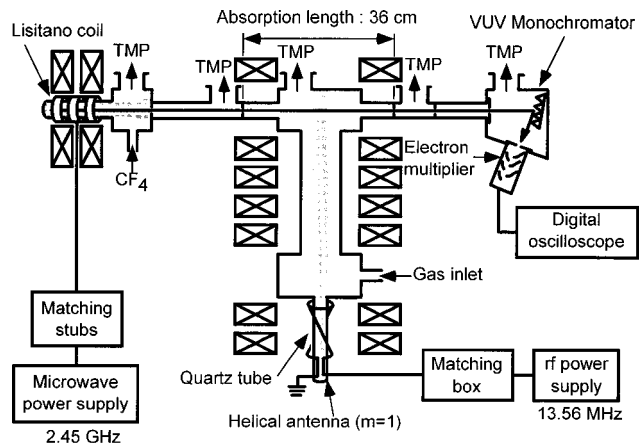


FIG. 2. Schematic of the experimental apparatus. The VUVAS system employs a compact ECR CF_4 plasma source and a VUV monochromator.

ber. Plasmas were produced in a quartz glass discharge tube of 3 cm diam. Various rf powers at 13.56 MHz were applied to a helical antenna wound around the discharge tube. The operating gas was pure CF_4 and C_4F_8 in the present experiment. The vacuum chamber was composed of a Pyrex glass tube (9 cm in diameter) and two stainless-steel observation chambers ($20 \times 20 \times 10$ cm). The plasmas were produced periodically with repetition rates of 5 Hz for CF_4 and 4 Hz for C_4F_8 . The discharge durations were 10 and 20 ms for CF_4 and C_4F_8 , respectively.

The system for VUVAS was installed in the downstream at a distance of approximately 50 cm from the end of the helical antenna. A compact electron-cyclotron resonance (ECR) plasma was employed as the light source for the absorption measurement. The operating gas of the ECR light source was pure CF_4 , and the fluorescence at 95.85 nm from the F atoms in the ECR plasma was used as the probe emission. A set of Helmholtz coil produced a divergent magnetic field of 875 G, which is resonant for a microwave power at a frequency of 2.45 GHz. The ignition of the plasma was obtained easily for low microwave powers (<10 W) and low gas pressures (<0.2 mTorr) by utilizing a Lisitano coil⁹ which was located outside of the quartz glass discharge tube. The light source ECR plasma was typically operated with a microwave power of 100 W and a gas pressure of 1 mTorr in the present experiment. The length of the ECR plasma along the line of vision for the absorption measurement was approximately 40 cm. The low-power, low-pressure discharge is helpful not only to construct a windowless transmission system for the probe emission but also to minimize radiation trapping (self-absorption) in the light source.

The transmission system for the probe emission was composed of stainless-steel vacuum tubes with no windows. Four stainless-steel plates with small slits were inserted into the vacuum tubes. The connection tube between the ECR and helicon plasma sources was differentially evacuated with a turbomolecular pump to prevent neutral particles from passing through. The probe emission was detected with a VUV monochromator (ARC, VM-502) and an electron multiplier tube. The wavelength resolution of the monochromator was adjusted at 0.28 nm. The output signal from the electron multiplier tube was recorded with a digital oscilloscope. The pressures in the monochromator and the electron multiplier tube were kept below 8×10^{-5} Torr by two-stage differential pumping. The absorption length of 36 cm was determined by the two stainless-steel plates attached to both sides of the helicon chamber. A uniform distribution was assumed for the F atom density in the helicon chamber since the lifetime of F atoms was much longer than the geometrical diffusion time determined by the chamber design. Since most of the F atoms were placed outside of the column of helicon plasma [the absorption length was much longer than the diameter of the plasma column (3 cm)], it was reasonably assumed that the equilibrium between the two sublevels of the ground state ($2p^5 2P_{3/2}^{\circ}$ and $2p^5 2P_{1/2}^{\circ}$) was determined by the F atom temperature (assumed to be 300 K in Fig. 3). Figure 3 shows the relation between the absorption at 95.85 nm and the total F atom density for the absorption length of $L=36$ cm, which was calculated by Eqs. (1) and (2). The

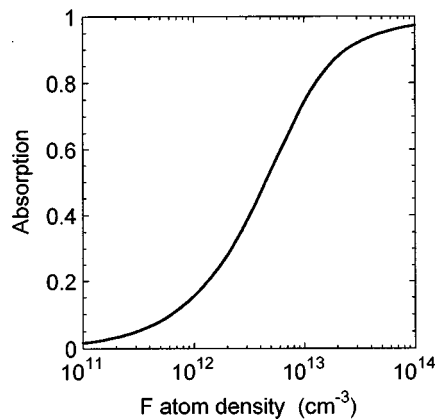


FIG. 3. Relation between the absorption at 95.85 nm and the total ground state F atom density, which is calculated by Eqs. (1) and (2). The F atom temperature in the ECR and helicon plasmas are assumed to be 400 and 300 K, respectively, and the radiation trapping effect in the ECR plasma is ignored.

radiation trapping (self-absorption) effect is ignored in Fig. 3, and Gaussian line shapes at 400 and 300 K are assumed for emitting F atoms in the light source and absorbing F atoms in the helicon plasma, respectively. Sensitive measurements are possible for F atom densities of the order of 10^{11} – 10^{13} cm^{-3} .

IV. RESULTS

In order to subtract the background dark current and the emission from the helicon plasma, measurement of the ab-

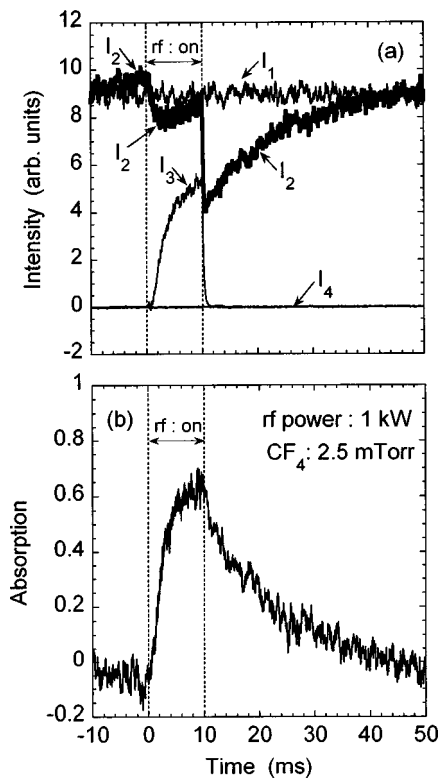


FIG. 4. (a) Typical signals observed in the four-step measurement, and (b) temporal variation of the absorption obtained from signals shown in (a). The rf power and the CF_4 gas pressure in the helicon plasma were 1 kW and 2.5 mTorr, respectively. The rf power was turned on during 0–10 ms.

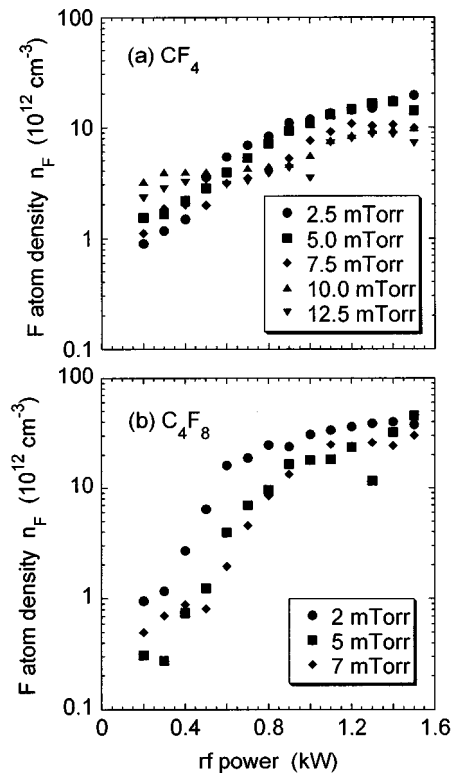


FIG. 5. rf power dependence of the absolute F atom density determined with VUVAS for (a) CF_4 and (b) C_4F_8 plasmas.

sorption was divided into four steps. First, only the light source (ECR) plasma was turned on and the emission intensity including the dark current was recorded (signal I_1). Second, both the helicon and ECR plasmas were turned on. The recorded signal in this step (signal I_2) consisted of the dark current, the emission from the helicon plasma, and the emission from the ECR plasma with absorption by F atoms in the helicon plasma. Third, only the helicon plasma was turned on and the emission intensity was recorded (signal I_3). Finally, the level of the dark current was recorded (signal I_4). Each of the four signals was averaged 500 times before recording with a digital oscilloscope to improve the signal-to-noise ratio. Typical signals are shown in Fig. 4(a) for a CF_4 gas pressure of 2.5 mTorr and a rf power of 1 kW. The rf power was turned on during 0–10 ms. The time response of the measurement was limited by the input resistor of the oscilloscope (1 M Ω), and was 200 μs in the present experiment. The incident emission intensity I_0 was obtained by subtracting the signal measured in the fourth step from that in the first step ($I_0 = I_1 - I_4$), while the transmitted intensity I_t was obtained by subtracting the signal measured in the third step from that in the second step ($I_t = I_2 - I_3$). The absorption $A = 1 - (I_t/I_0)$ was thus obtained from the four-step measurement as shown in Fig. 4(b). The temporal variation of the F atom density was readily obtained from Figs. 3 and 4(b).

Figure 5 shows the rf power dependence of the F atom density measured in the CF_4 and C_4F_8 plasmas. The range of the absolute F atom density was on the order of 10^{11} – 10^{13} cm^{-3} . For low rf powers (< 500 W), the F atom density in the C_4F_8 plasma was lower than that in the CF_4 plasma.

TABLE I. Estimation of the measurement error.

Source	Error
Transition probability	$\pm 25\%$
F atoms in the connecting section	+30%
Signal-to-noise ratio	$\pm 10\%$
Spectral broadening of the absorption line	+30%
Line shape of the probe emission	$\pm 15\%$

However, the increase in the F atom density in the C_4F_8 plasma was steeper than that in the CF_4 plasma. As a result, the F atom density in the C_4F_8 plasma was higher than that in the CF_4 plasma for high rf powers (>1 kW). It is noted that the CF_x radical density was approximately one-order higher in the C_4F_8 plasma than in the CF_4 plasma.^{10,11} The details of the reaction kinetics of F atoms in the CF_4 and C_4F_8 plasmas have been reported previously.^{6,7}

V. DISCUSSION

A. Sources of the measurement error

The measurement error of the present method arises from various sources summarized in Table I. The first source of the error is the uncertainty contained in the transition probability listed in literature.¹² According to the literature, an error of 25% is possibly contained in the transition probability used in the present study ($1.25 \times 10^8 \text{ s}^{-1}$ for 95.85 nm).^{12,13} The second source of the error is due to the fact that no windows can be used for the emission at 95.85 nm. Although both sides of the helicon chamber are differentially evacuated with turbomolecular pumps, there is a considerable amount of F atoms in the connection tubes, which contributes to the absorption of the probe emission. The gas pressures in the connection tubes were ~ 0.5 mTorr in both sides when the gas pressure in the helicon chamber was 2.5 mTorr. Hence, it is possible that the F atom densities in the connection tubes are approximately one-fifth of that in the helicon chamber. If the absorption length in the connection tubes of both sides is assumed to be 70 cm, the overestimation for the F atom density in the helicon chamber becomes approximately 40%. It is noted here that the F atoms produced in the helicon plasma did not reach the ECR plasma, which was confirmed by measuring a visible emission from FI in the ECR plasma with and without the operation of the helicon plasma. The assumption of a uniform spatial distribution for the F atom density in the helicon chamber is fairly reasonable, since the lifetime of F atoms is much longer than the geometrical diffusion time determined by the chamber design. The third source of the error is the random noise superposed on the signals from I_1 to I_4 . Averaging the signals for 500 times suppresses the random noise, and the uncertainty due to the noise is smaller than $\pm 10\%$.

The fourth and fifth sources of the measurement error are due to the assumptions on the spectral distributions of absorbing and emitting F atoms. A Gaussian profile (Doppler broadening) characterized by a F atom temperature of 300 K was assumed for the spectral distribution of absorbing F atoms in the helicon plasma. The temperature of 300 K was assumed by referring to an experimental result that the rota-

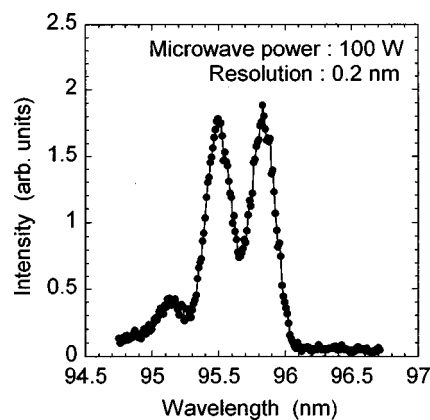


FIG. 6. Spectrum of the VUV emission from F atoms in the ECR light source plasma operated with a microwave power of 100 W and a CF_4 gas pressure of 1 mTorr. The wavelength resolution of the monochromator was 0.2 nm.

tional temperature of CF radicals, which was determined from an excitation spectrum in the LIF measurements, was 300–380 K in the plasma column. Since most of the F atoms were placed outside of the plasma column in the present experimental configuration, the temperature of 300 K may be a reasonable assumption. According to the sensitivity analysis based on the uncertainty in the temperature of absorbing F atoms, the absolute F atom density shown in the present article becomes ~ 0.7 times smaller if we assume a temperature of 400 K for absorbing F atoms. The error due to the assumption on the temperature of emitting F atoms in the ECR plasma can also be evaluated by the sensitivity analysis, and is $\pm 15\%$ corresponding to the temperature of 400 ± 100 K. However, the error due to the distortion of the spectral distribution of the probe emission is difficult to estimate. Possibly, the spectral distribution of the probe emission may be distorted considerably from the Gaussian profile due to radiation trapping (self-absorption) in the light source plasma. Strongly distorted spectral distributions have been observed in VUV emissions from H (Lyman α line)^{14,15} and O atoms.¹⁶ In the present work, the influence of radiation trapping was minimized by choosing the probe emission at 95.85 nm as described in the next section.

B. Influence of radiation trapping

Figure 6 shows the VUV emission spectrum from F atoms in the ECR plasma operated with a microwave power of 100 W and a CF_4 gas pressure of 1 mTorr. Because of the poor wavelength resolution of the monochromator (0.2 nm in this measurement), the emissions at 95.48 and 95.55 nm are overlapped in the middle peak around 95.5 nm. Table II

TABLE II. Transition probability and statistical weights for the four transition lines between $2p^5^2P^\circ$ and $3s^2P$.

λ_0 (nm)	A_{21} (10^8 s^{-1})	g_2	g_1	$g_2 A_{21}$ (relative)
95.19	2.56	2	4	1.0
95.48	6.34	4	4	5.1
95.55	5.01	2	2	2.0
95.85	1.25	4	2	1.0

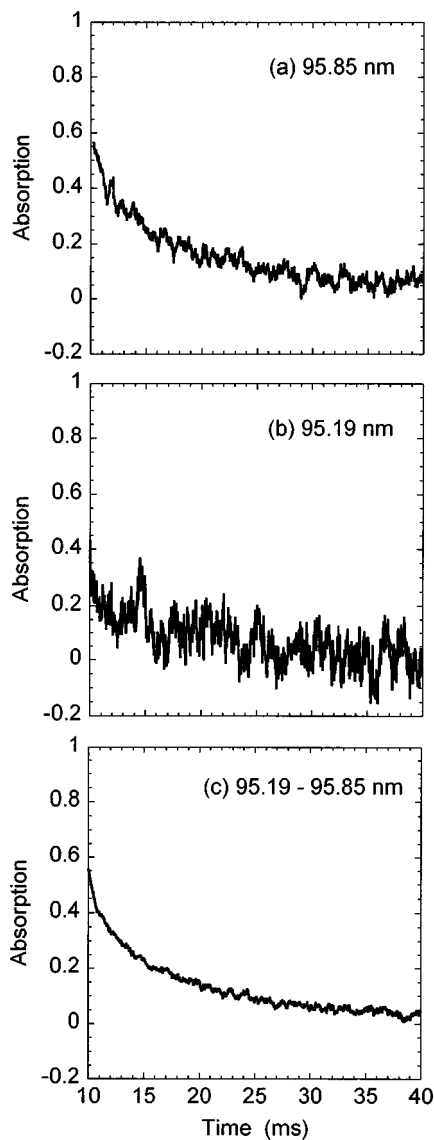


FIG. 7. Comparison of the absorption for three different probe emissions at (a) 95.85 nm, (b) 95.19 nm, and (c) 95.19–95.85 nm. The wavelength resolution of the monochromator was set at 1.5 nm in (c).

shows the transition probabilities and the statistical weights for the four transition lines shown in Fig. 1.¹² According to a simple prediction that the emission intensity is roughly proportional to $g_2 A_{21}$, similar intensities are expected for the emissions at 95.19 and 95.85 nm (the intensity ratio of 1.0:1.0). However, the emission intensity at 95.19 nm observed experimentally is approximately one-fifth of the intensity at 95.85 nm. The experimental result shows the similar emission intensities at 95.85 nm and a peak around 95.5 nm (overlap of 95.48 and 95.55 nm), which also contradicts a simple prediction from Table II that the sum of the emission intensities at 95.48 and 95.55 nm is much larger than the intensity at 95.85 nm (the intensity ratio of 1.0:7.1). These results suggest that the emissions at 95.19 and 95.48 nm are absorbed strongly in the light source ECR plasma. This may be because the lower energy level of these transitions is the lower ground state ($2p^{52}P_{3/2}^{\circ}$). The self-absorption at 95.85 nm is expected to be smaller since the lower energy level of the transition is the higher ground state ($2p^{52}P_{1/2}^{\circ}$). The

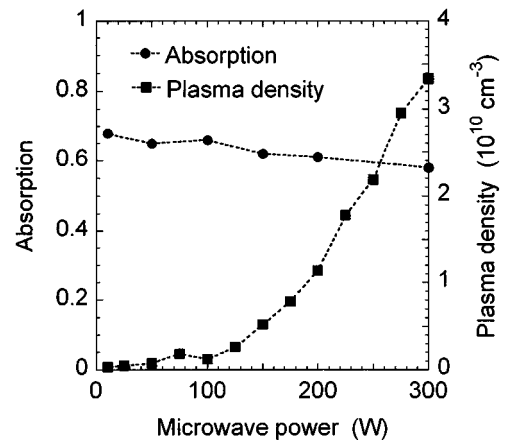


FIG. 8. Absorption in the helicon CF_4 plasma (1 kW, 2.5 mTorr) as a function of the microwave power applied to the ECR light source plasma.

small transition probability for 95.85 nm is also a good condition for the small self-absorption.

Figure 7 shows temporal variations of the absorption in the helicon plasma measured with three different probe emissions at 95.85, 95.19, and 95.19–95.85 nm. The helicon plasma was operated with a rf power of 1 kW and a CF_4 gas pressure of 2.5 mTorr. Since the signal-to-noise ratio for the measurement at 95.19 nm was low, the comparison was restricted to the afterglow phase (the rf power was terminated at 10 ms in Fig. 7). In Fig. 7(c), the wavelength resolution of the monochromator was set at 1.5 nm to detect the whole of the four emissions. Since the population at the lower ground state ($2p^{52}P_{3/2}^{\circ}$) is ~ 14 times higher than that at the higher ground state ($2p^{52}P_{1/2}^{\circ}$) when assuming the Boltzmann distribution at 300 K between the two sublevels, the absorption at 95.19 nm is expected to be greater than that at 95.85 nm. However, the experimental result contradicted this simple prediction, and the absorption at 95.19 nm was slightly smaller than that at 95.85 nm. In addition, when we used the whole of the four emissions as the probe emission [Fig. 7(c)], the absorption was almost the same as that at 95.85 nm. This result suggests that the absorption was mainly determined by the emissions at 95.55 and 95.85 nm, and the emissions at 95.19 and 95.48 nm negligibly contributed to the absorption. If the spectral distribution of the probe emission is distorted from the Gaussian profile due to the radiation trapping (self-absorption) effect in the light source plasma, the absorption in the helicon plasma may become much smaller.¹⁴ Therefore, from the experimental results, we can suppose that the spectral distributions of the emissions at 95.19 and 95.48 nm from the ECR plasma were strongly distorted. Hence, it is difficult to determine the absolute F atom density with the emissions at 95.19 and 95.48 nm.

In order to examine the degree of radiation trapping at 95.85 nm, the absorption in the helicon plasma was measured for various microwave powers applied to the ECR light source plasma. The result is shown in Fig. 8, together with the plasma density of the ECR plasma measured with a heated Langmuir probe.¹⁷ The plasma densities were 3.1×10^8 – $3.3 \times 10^{10} \text{ cm}^{-3}$ for microwave powers of 10–300 W.

Accordingly, the F atom density in the ECR plasma probably varied in a wide range, which may result in the change in the degree of radiation trapping. The stronger spectral distortion due to radiation trapping makes the absorption in the helicon plasma smaller. As shown in Fig. 8, a slight decrease in the absorption was observed for microwave powers higher than 150 W. For microwave powers lower than 100 W, the absorption was almost constant. Therefore, we used the ECR light source plasma for a microwave power of 100 W, in which the influence of radiation trapping at 95.85 nm on the determination of the absolute F atom density is probably negligible.

ACKNOWLEDGMENTS

This work was supported by the Tatematsu Foundation and by a Grant-in-Aid for Scientific Research from the Ministry of Education, Science, Sports, and Culture of Japan.

¹J. W. Coburn and M. Chen, *J. Appl. Phys.* **51**, 3134 (1980).

²Y. Kawai, K. Sasaki, and K. Kadota, *Jpn. J. Appl. Phys., Part 2* **36**, L1261 (1997).

³K. Nakamura, K. Segi, and H. Sugai, *Jpn. J. Appl. Phys., Part 2* **36**, L439 (1997).

⁴A. Tserepi, W. Schwarzenbach, J. Derouard, and N. Sadeghi, *J. Vac. Sci. Technol. A* **15**, 3120 (1997).

⁵K. Sasaki, Y. Kawai, and K. Kadota, *Appl. Phys. Lett.* **70**, 1375 (1997).

⁶K. Sasaki, Y. Kawai, C. Suzuki, and K. Kadota, *J. Appl. Phys.* **82**, 5938 (1997).

⁷K. Sasaki, Y. Kawai, C. Suzuki, and K. Kadota, *J. Appl. Phys.* **83**, 7482 (1998).

⁸A. G. Mitchell and M. W. Zemansky, *Resonance Radiation and Excited Atoms* (Cambridge University Press, Cambridge, England, 1961), p. 92.

⁹G. Lisitano, R. A. Ellis, W. M. Hooke, and T. H. Stix, *Rev. Sci. Instrum.* **39**, 295 (1968).

¹⁰C. Suzuki, K. Sasaki, and K. Kadota, *J. Appl. Phys.* **82**, 5321 (1997).

¹¹C. Suzuki, K. Sasaki, and K. Kadota, *J. Vac. Sci. Technol. A* **16**, 2222 (1998).

¹²D. C. Morton, *Astrophys. J., Suppl. Ser.* **77**, 119 (1991).

¹³W. L. Wiese and G. A. Martin, in *CRC Handbook of Chemistry and Physics, 70th ed.*, edited by R. C. Weast (CRC, Cleveland, OH, 1989-1990).

¹⁴K. Tachibana, *Jpn. J. Appl. Phys., Part 1* **33**, 4329 (1994).

¹⁵J. Amorim, J. Loureiro, G. Bavarian, and M. Touzeau, *J. Appl. Phys.* **82**, 2795 (1997).

¹⁶G. Gousset, P. Panafieu, M. Touzeau, and M. Vialle, *Plasma Chem. Plasma Process.* **7**, 409 (1987).

¹⁷N. Takada, D. Hayashi, K. Sasaki, and K. Kadota, *J. Plasma Fusion Res.* **74**, 758 (1998) (in Japanese).